

Triplet Organometallic Reactivity under Ambient Conditions: An Ultrafast UV Pump/IR Probe Study

Preston T. Snee, Christine K. Payne, Kenneth T. Kotz, Haw Yang,[‡] and Charles B. Harris*

Contribution from the Department of Chemistry, University of California, Berkeley, California, 94720, and Chemical Sciences Division, Ernest Orlando Lawrence Berkeley, National Laboratory, Berkeley, California, 94720

Received June 29, 2000

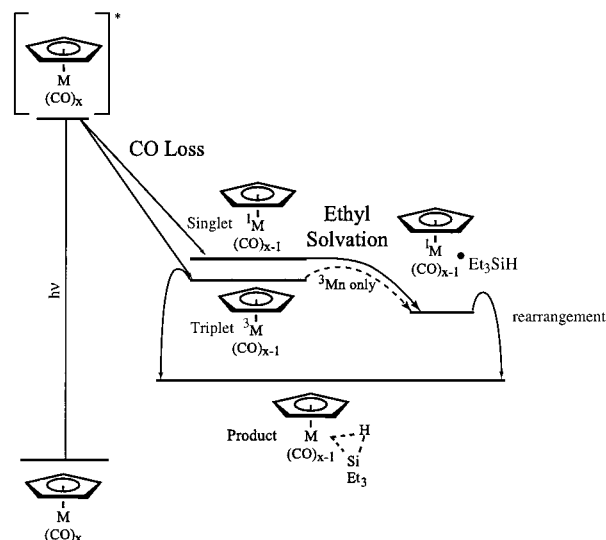
Abstract: The reactivity of triplet 16-electron organometallic species has been studied in room-temperature solution using femtosecond UV pump IR probe spectroscopy. Specifically, the Si–H bond-activation reaction of photogenerated triplet $\text{Fe}(\text{CO})_4$ and triplet $\text{CpCo}(\text{CO})$ with triethylsilane has been characterized and compared to the known singlet species $\text{CpRh}(\text{CO})$. The intermediates observed were studied using density functional theory (DFT) as well as ab initio quantum chemical calculations. The triplet organometallics have a greater overall reactivity than singlet species due to a change in the Si–H activation mechanism, which is due to the fact that triplet intermediates coordinate weakly at best with the ethyl groups of triethylsilane. Consequently, the triplet species do not become trapped in alkyl-solvated intermediate states. The experimental results are compared to the theoretical calculations, which qualitatively reproduce the trends in the data.

I. Introduction

Bond activation by coordinatively unsaturated organometallic species is a subject of great interest in the chemical sciences.¹ One interesting, yet relatively unexplored, aspect of bond activation is the effect of the reactants' electronic state on the reaction mechanism. In our earlier publications on Si–H bond activation, we characterized the reactivity of singlet as well as previously unknown triplet intermediates formed upon photolysis of $\text{CpV}(\text{CO})_4$ and $\text{CpMn}(\text{CO})_3$ ($\text{Cp} = \text{C}_5\text{H}_5$) in triethylsilane solution, as summarized in Scheme 1.^{2–4} Contrary to the general conception that a triplet species has a slower reactivity than a singlet species due to spin-crossing barriers, these triplet intermediates formed the bond-activated product on a time scale faster than that of their iso-electronic singlet counterparts.

In the present investigation, the Si–H bond-activation reaction using the d^8 organometallic compounds $\text{CpCo}(\text{CO})_2$, $\text{CpRh}(\text{CO})_2$, and $\text{Fe}(\text{CO})_5$ in triethylsilane has been studied. These species form intermediates in different spin states,^{5–10} and previous investigations have shown that these compounds are capable of photochemically activating Si–H bonds.^{11–14} In this

Scheme 1. Si–H Bond-Activation Mechanism of $\text{CpV}(\text{CO})_4$ and $\text{CpMn}(\text{CO})_3$, from Refs 2, 3



* To whom correspondence should be addressed.

[‡] Present address: Harvard University, Chemical Laboratories, Box 225, 12 Oxford St., Cambridge, MA 02138.

(1) Arndsten, B. A.; Bergman, R. G.; Mobley, T. A.; Peterson, T. H. *Acc. Chem. Res.* **1995**, *28*, 154.

(2) Snee, P. T.; Yang, H.; Kotz, K. T.; Payne, C. K.; Harris, C. B. *J. Phys. Chem. A* **1999**, *103*, 10426.

(3) Yang, H.; Asplund, M. C.; Kotz, K. T.; Wilkens, M. J.; Frei, H.; Harris, C. B. *J. Am. Chem. Soc.* **1998**, *120*, 10154.

(4) Yang, H.; Kotz, K. T.; Asplund, M. C.; Harris, C. B. *J. Am. Chem. Soc.* **1997**, *119*, 9564.

(5) Barnes, L. A.; Rosi, M.; Bauschlicher, C. W. *J. Chem. Phys.* **1990**, *94*, 2031.

(6) Barton, T. J.; Grinter, R.; Thomson, A. J.; Davies, B.; Poliakov, M. *J. Chem. Soc., Chem. Commun.* **1977**, 841.

(7) Burdett, J. K. *J. Chem. Soc., Faraday Trans. 2* **1974**, *70*, 1599.

(8) Daniel, C.; Benard, M.; Dedieu, A.; Wiest, R.; Veillard, A. *J. Phys. Chem.* **1984**, *88*, 4805.

(9) Ziegler, T.; Tschinke, V.; Fan, L.; Becke, A. D. *J. Am. Chem. Soc.* **1989**, *111*, 9177.

(10) Siegbahn, P. E. M. *J. Am. Chem. Soc.* **1996**, *118*, 1487.

paper we compare the reactivity of these photogenerated singlet and triplet species in triethylsilane to understand how the organometallic electronic state affects the Si–H bond-activation mechanism.

The chemistry of $\text{CpCo}(\text{CO})_2$ has been extensively studied by several groups.^{15–17} Using theoretical calculations, Siegbahn

(11) Oliver, A. J.; Graham, W. A. G. *Inorg. Chem.* **1971**, *10*, 1.

(12) Jetz, W.; Graham, W. A. G. *Inorg. Chem.* **1971**, *10*, 4.

(13) $^3\text{Fe}(\text{CO})_4$ is also known to activate H_2 . See Sweany, R. *J. Am. Chem. Soc.* **1981**, *103*, 2410.

(14) The results from the DFT calculations indicate that the Si–H bond is fully or almost fully activated in these product species.

(15) Rest, A. J.; Whitwell, I.; Graham, W. A. G.; Hoyano, J. K.; McMaster, A. D. *J. Chem. Soc., Dalton Trans.* **1987**, 1181.

(16) Wasserman, E. P.; Moore, C. B.; Bergman, R. G. *Science* **1992**, *255*, 315.

(17) Bengali, A. A.; Bergman, R. G.; Moore, C. B. *J. Am. Chem. Soc.* **1995**, *117*, 3879.

has shown that the photoproduct CpCo(CO) has a triplet electronic ground state.¹⁰ Theoretical calculations have also shown that triplet organometallic species generally have much weaker interactions with alkanes compared to alkane/singlet interactions.^{10,17–20} These results are consistent with the experimental observations of Bengali et al., which show that triplet CpCo(CO) is unable to activate C–H bonds and does not coordinate strongly with alkanes.¹⁷ There appear, however, to be no kinetic studies of the Si–H activation of CpCo(CO)₂. We have studied the photolysis of CpCo(CO)₂ in triethylsilane solution and compare the reactivity to that of CpRh(CO)₂. The difference in the rate of reaction between the singlet and triplet intermediates of these species highlights the effect of spin state on reactivity.

The photochemical reaction dynamics of Fe(CO)₅ has also been the subject of thorough study in the literature.^{21–25} It has been established that both singlet and triplet Fe(CO)₄ are formed upon photolysis of Fe(CO)₅ in the gas phase and in matrix isolation studies; likewise Burkey and Nayak have shown that triplet Fe(CO)₄ is formed in room-temperature alkane/phosphine solution.^{26,27} While other authors have suggested that the unusual reaction dynamics observed by Burkey and Nayak are due in part to singlet Fe(CO)₄,²⁸ the present study finds no evidence of singlet Fe(CO)₄ formation in room-temperature solution on the ultrafast time scale. We will show that the photochemistry of Fe(CO)₅ is important as an example of triplet reactivity.

Many authors have found that a triplet's reactivity is slower than that of a singlet species, such as in the case of the gas-phase recombination studies of Fe(CO)_x ($x = 2–4$) with CO and Fe(CO)₅.^{24,29} This has been attributed to the fact that, in the case of a spin nonconserving reaction, the formally forbidden spin crossover process connecting reactants to products may act as an additional reaction barrier. While a disparity does exist between the reactivity of singlet and triplet organometallic intermediates with triethylsilane, the triplet species is the most reactive. A detailed mechanistic analysis is necessary to understand the reversal of the trend in the singlet/triplet reactivity. The experimental results are compared to ab initio and density functional theory (DFT) calculations, which provide valuable insight into the reaction barriers as well as the quantum mechanical (spin–orbit) coupling between the spin states. The previous investigations of CpMn(CO)₃ and CpV(CO)₄ augment the present work.

II. Methods

Sample Synthesis/Sample Handling. The compounds CpCo(CO)₂ and Fe(CO)₅ were purchased from Strem, Inc. and used without further purification. Anhydrous heptane was purchased from Aldrich, and triethylsilane was purchased from Gelest, Inc. All samples were prepared under nitrogen atmosphere in an airtight, liquid IR flow cell from Harrick Scientific Corporation using a 250 μm cell thickness.

(18) Blomberg, M. R. A.; Siegbahn, P. E. M.; Svensson, M. *J. Am. Chem. Soc.* **1992**, *114*, 6095.

(19) Siegbahn, P. E. M.; Svensson, M. *J. Am. Chem. Soc.* **1994**, *116*, 10124.

(20) Carroll, J. J.; Weisshaar, J. C.; Haug, K. L.; Blomberg, M. R. A.; Siegbahn, P. E. M.; Svensson, M. *J. Phys. Chem.* **1995**, *99*, 13955.

(21) Poliakoff, M.; Turner, J. J. *J. Chem. Soc., Dalton Trans.* **1974**, 2276.

(22) Poliakoff, M.; Weitz, E. *Acc. Chem. Res.* **1987**, *20*, 408.

(23) Poliakoff, M. *Spectrochim. Acta* **1987**, *43A*, 217.

(24) Ryther, R. J.; Weitz, E. *J. Phys. Chem.* **1991**, *95*, 9841–9852.

(25) Leadbeater, N. *Coord. Chem. Rev.* **1999**, *188*, 35.

(26) Nayak, S. K.; Farrell, G. J.; Burkey, T. J. *Inorg. Chem.* **1994**, *33*, 2236.

(27) Nayak, S. K.; Burkey, T. J. *Inorg. Chem.* **1992**, *31*, 1125.

(28) Trushin, S. A.; Fuss, W.; Kompa, K. L.; Schmid, W. E. *J. Phys. Chem. A* **2000**, *104*, 1997.

(29) Ouderkerk, A. J.; Weitz, E. *J. Chem. Phys.* **1983**, *79*, 1089.

The concentrations of CpCo(CO)₂ and Fe(CO)₅ were approximately 8 and 7 mM, respectively, in alkane and triethylsilane solution. The long-time spectra in Figure 2 was taken using a one-to-one equivalent of Fe(CO)₅ (5 mM) and triethylsilane in heptane solution to suppress the formation of the di-substituted product due to secondary photolysis. The photolysis of CpMn(CO)₃ in *n*-pentane has been studied previously, although the results were not reported earlier.^{3,4} These photochemical studies used a 18.5 mM solution of CpMn(CO)₃ and *n*-pentane in a 950 μm cell.

The compound CpRh(CO)₂ was synthesized from [RhCl(CO)₂]₂ and TiC₅H₅ using a modification of the method of Knight.³⁰ The reactants were mixed in petroleum ether in the dark for 4 days. After removing the solvent, the product was purified with an activated alumina column using triethylsilane as the effluent. The sample purity was established using standard spectroscopic methods. The ultrafast spectra of this compound were taken using a 150 μm cell thickness.

Femtosecond Infrared Spectroscopy. Details of the femtosecond IR (fs-IR) spectrometer setup have been published elsewhere.³¹ The output of a Ti:sapphire oscillator was amplified in two prism-bored dye-cell amplifiers,³² which were pumped by the output of a frequency-doubled 30 Hz Nd:YAG laser. The amplified light centered at ~ 810 nm was then split into three beams. One beam was further amplified to give 70-fs, 7- μJ pulses while the other two were focused into two sapphire windows to generate white light continuum. Desired wavelengths of the white light were selected by two band-pass (BP) filters with full-width-half-maximum (fwhm) of 10 nm, and further amplified by three-stage dye amplifiers to produce light pulses centered at 590 or 650 nm, as well as 690 nm. In this study, the excitation pulses of 295 or 325 nm were generated by frequency doubling the 590- or 650-nm light, respectively. The resulting UV photons (with energy of ~ 4 $\mu\text{J}/\text{pulse}$) were focused into a disk of ~ 200 - μm diameter at the sample to initiate the chemical reactions. The required time delay between a pump pulse and a probe pulse was achieved by guiding the pump beam through a variable delay line.

The broadband, ultrafast probe pulses centered at 5 μm were generated by mixing the 690 nm beam with the 810 nm beam. The resulting ~ 5 - μJ IR pulses having temporal fwhm of about 70 fs and spectral bandwidth of about 200 cm^{-1} were split into a signal and a reference beam. Both the signal beam and the reference beam were then focused into an astigmatism-corrected spectrographic monochromator (Spectra-Pro-150, Acton Research Corp., 150 g/mm , 4.0 μm blazed) to form two spectrally resolved images on a focal-plane-array (FPA) detector. The two frequency resolved images were digitized by two windows of 12 \times 200 pixels, which allowed simultaneous normalization of a 70 cm^{-1} spectrum. The sensing chip of the detector was an engineer grade, 256 \times 256-element HgCdTe (MCT) matrix of dimensions 1.28 \times 1.28 cm. The typical spectral and temporal resolution for this setup are 4 cm^{-1} and 300 fs, respectively. The polarizations of the pump and the probe pulse were set at the magic angle (54.7°) to ensure that all signals were due to population dynamics. A broad, wavelength-independent background signal from CaF₂ windows has been subtracted from the transient spectra and kinetic traces.

Quantum Chemical Modeling. To compare single-point energies consistently, all calculations were carried out using DFT-optimized geometries. The hybrid B3LYP functional was used for the DFT calculations with the Jaguar package.^{33–35} This functional has been shown to give very good results for transition metal complexes.^{36,37} The basis set consisted of the 6-31G** basis functions for H, C, O, and Si,^{38,39} and the Los Alamos effective core potential (ECP) for V,

(30) Knight, J.; Mays, J. *J. Chem. Soc. A* **1970**, 654.

(31) Lian, T.; Bromberg, S. E.; Asplund, M. C.; Yang, H.; Harris, C. B. *J. Phys. Chem.* **1996**, *100*, 11994.

(32) Bethune, D. S. *Appl. Opt.* **1981**, *20*, 1987.

(33) Becke, A. D. *J. Chem. Phys.* **1993**, *98*, 5648.

(34) Lee, C.; Yang, W.; Parr, R. G. *Phys. Rev.* **1988**, *B41*, 785.

(35) Stephens, P. J.; Devlin, F. J.; Chabalowski, C. F.; Frisch, M. J. *J. Phys. Chem.* **1994**, *98*, 11623.

(36) Ricca, A.; Bauschlicher C. W. *Theor. Chim. Acta* **1995**, *92*, 123.

(37) Glukhovtsev, M. N.; Bach, R. D.; Nagel, C. J. *J. Phys. Chem.* **1997**, *101*, 316.

(38) Hehre, W. J.; Ditchfield, R.; Pople, J. A. *J. Chem. Phys.* **1972**, *56*, 2257.

Mn, Fe, Co, and Rh with the outermost core orbitals included in the valence description.⁴⁰ All geometry optimizations were followed by a frequency analysis to make certain that the optimized geometries were at a minimum.

To determine the ground spin state of all of the intermediate species under study, second-order perturbation theory calculations of the complete active space multiconfigurational self-consistent field wave function (pt2-mcscf) were performed for the singlet and triplet species. These *ab initio* calculations were carried out using the GAMESS-US package,^{41,42} using the lan12dz basis set.^{40,43–45} The active space of the casscf calculations consisted of 10 occupied and unoccupied d-type orbitals, while the perturbative calculations excluded only the core electrons.⁴⁶ The coupling (spin–orbit) strength was calculated at the ground-state triplet geometry using the method of corresponding orbitals.⁴⁷ As it is computationally unfeasible to calculate the full Breit–Pauli spin–orbit Hamiltonian for the optimized mcscf wave function, the two-electron component of the operator is removed, and an approximate metal charge (Z_{eff}) is used. The Z_{eff} at the metal center described by Koseki et al. was used to calculate the spin–orbit coupling, again using the lan12dz basis set.⁴⁸

For computational efficiency, the neat alkane (or ethyl moiety of triethylsilane) interaction and Si–H interaction with the singlet/triplet organometallic complexes was modeled using C_2H_6 or SiH_3CH_3 , respectively. The binding strengths of the singlet species were also calculated at the MP2 level of theory using the counterpoise method to account for basis set superposition error^{49,50} including DFT/B3LYP zero-point energy corrections.

To describe the trends seen in the reactivity of the triplet species $\text{CpV}(\text{CO})_3$, $\text{Fe}(\text{CO})_4$, and $\text{CpCo}(\text{CO})$ in triethylsilane, the DFT potential energy curves for these organometallic species with SiH_3CH_3 were calculated by fixing the metal–Si bond lengths (R) of the organometallic complexes and subsequently optimizing the remaining geometric parameters. This was done for both singlet and triplet organometallic fragments at various values of R near the singlet–triplet crossing region. This type of analysis builds an approximate potential energy surface for the bond-activation reaction as a function of the metal–Si distance, although the actual activation coordinate is more complex due to the high dimensionality of the dynamics.

III. Results

The IR spectra in the CO-stretching region are presented in the form of difference absorbance spectra in which positive bands indicate the appearance of new species while negative bands (bleaches) represent the depletion of parent molecules. Gaps appear in some spectra where the parent compound has strong absorptions, as very little IR signal penetrates the sample in these frequency regions.

A. Photolysis of $\text{CpCo}(\text{CO})_2$, $\text{Fe}(\text{CO})_5$, and $\text{CpMn}(\text{CO})_3$ in Alkane Solution.

The photolysis of $\text{CpCo}(\text{CO})_2$, $\text{Fe}(\text{CO})_5$,

(39) Francl, M. M.; Petro, W. J.; Hehre, W. J.; Binkley, J. S.; Gordon, M. S.; Defrees, D. J.; Pople, J. A. *J. Chem. Phys.* **1982**, *77*, 3654.

(40) Hay, P. J.; Wadt, W. R. *J. Chem. Phys.* **1985**, *82*, 299.

(41) Schmidt, M. W.; Baldridge, K. K.; Boatz, J. A.; Elbert, S. T.; Gordon, M. S.; Jensen, J. H.; Koseki, S.; Matsunaga, N.; Nguyen, K. A.; Su, S.; Windus, T. L.; Dupuis, M.; Montgomery, J. A. *J. Comput. Chem.* **1993**, *14*, 1347.

(42) Nakano, H. *J. Chem. Phys.* **1993**, *99*, 7983.

(43) Dunning, T. H.; Hay, P. J. *Methods of Electronic Structure Theory*; Plenum: New York, 1977; Vol. 2.

(44) Hay, P. J.; Wadt, W. R. *J. Chem. Phys.* **1985**, *82*, 270.

(45) Hay, P. J.; Wadt, W. R. *J. Chem. Phys.* **1985**, *82*, 284.

(46) The singlet–triplet splittings and binding strengths have been reported for $\text{CpV}(\text{CO})_3$ and $\text{CpMn}(\text{CO})_2$; however, a change in the basis set, as well as the increase of the perturbative active space, has altered the results to a small extent.

(47) The method used optimized ground-state core orbitals for the ground- and excited-state casscf optimization. See Lengsfeld, B. H.; Jafri, J. A.; Phillips, D. H. *J. Chem. Phys.* **1981**, *74*, 6849.

(48) Koseki, S.; Schmidt, M. W.; Gordon, M. S. *J. Phys. Chem. A* **1998**, *102*, 10430.

(49) Boys, S. F.; Bernardi, F. *Mol. Phys.* **1970**, *19*, 553.

(50) Liu, B.; McLean, A. D. *J. Chem. Phys.* **1973**, *59*, 4557.

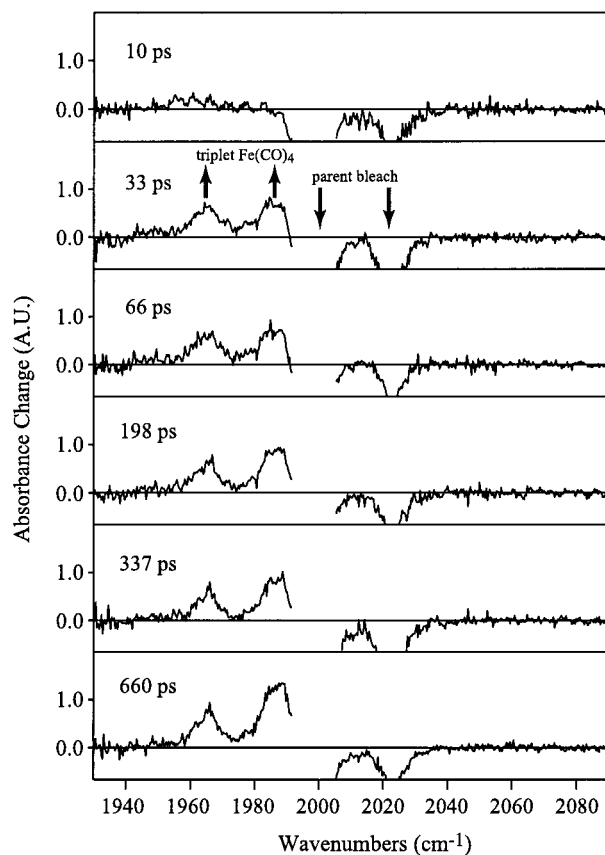
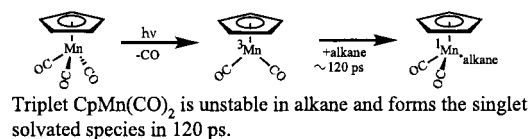
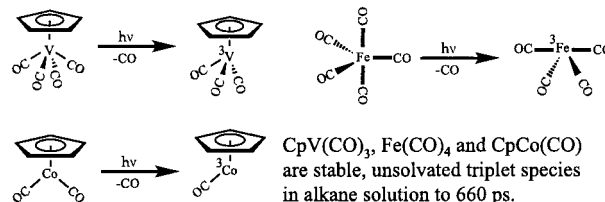


Figure 1. Transient difference spectra in the CO-stretching region for $\text{Fe}(\text{CO})_5$ in neat heptane at 10, 33, 66, 198, 337, and 660 ps following 295-nm UV photolysis. There is no evidence for the formation of $\text{Fe}(\text{CO})_3$ or singlet $\text{Fe}(\text{CO})_4$.

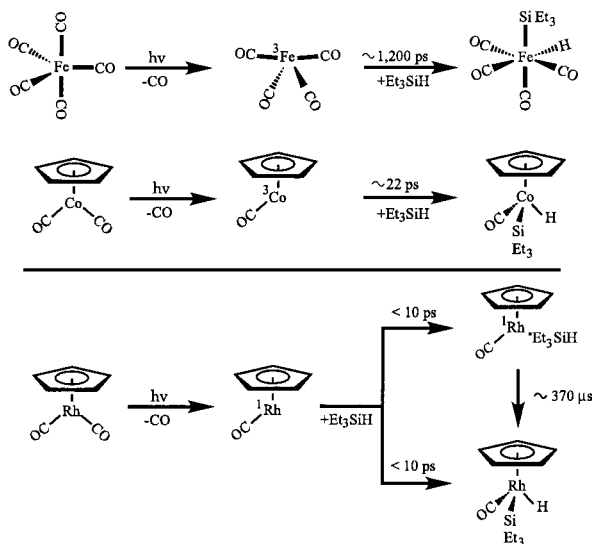
Scheme 2. Photochemistry of the Triplet Species $\text{CpV}(\text{CO})_3$, $\text{Fe}(\text{CO})_4$, $\text{CpCo}(\text{CO})$ and $\text{CpMn}(\text{CO})_2$ in Alkane Solution



and $\text{CpMn}(\text{CO})_3$ in alkane solution was studied. The photochemical studies of $\text{CpV}(\text{CO})_4$ in heptane were reported in ref 2 and the results for all of the organometallic species are summarized in Scheme 2. These results are used in the Discussion to compare the reactivity of singlet and triplet species in alkane and triethylsilane solution.

Upon 325-nm photolysis of $\text{CpCo}(\text{CO})_2$ in heptane solution, a single monocarbonyl peak appears at 1990 cm^{-1} on a time scale of 12 ± 2 ps and remains constant to 660 ps. As shown in Figure 1, the 295-nm photolysis of $\text{Fe}(\text{CO})_5$ results in the formation of instantaneous parent bleaches and the 26 ± 12 -ps formation of a new photoproduct absorbing at 1965 cm^{-1} and what appear to be two overlapped bands centered at 1987 cm^{-1} . This photoproduct appears to be stable to 660 ps.⁵¹ The rise times of these iron and cobalt species may be attributed to

Scheme 3. Photochemical Reactions of $\text{Fe}(\text{CO})_5$, $\text{CpCo}(\text{CO})_2$, and $\text{CpRh}(\text{CO})_2$ Observed within 660 ps in Triethylsilane Solution^a



^a The decay time scale of the ethyl moiety of $\text{CpRh}(\text{CO})$ in triethylsilane is estimated from ref 69.

vibrational relaxation of the initially hot photoproduct due to the slight broadening and blue-shifting of the photoproduct peak at early times.^{52–54} The assignments of these photogenerated intermediates are given in the Discussion.

The dynamics of photogenerated singlet and triplet $\text{CpMn}(\text{CO})_2$ in *n*-pentane had been studied during the earlier triethylsilane studies; however, the results were not reported. Following excitation at 295 nm, it was found that the triplet species is unstable in *n*-pentane and decays with a time constant of $\tau = 119 \pm 5$ ps. The loss of the triplet intermediate results in the formation of the singlet alkane-solvated species as shown in Scheme 2. The published value of the decay of the triplet species in triethylsilane ($\tau = 105$ ps) is similar.³

B. Activation of the Silicon–Hydrogen Bond of Et_3SiH by $\text{CpCo}(\text{CO})_2$, $\text{CpRh}(\text{CO})_2$, and $\text{Fe}(\text{CO})_5$. The activation of the Si–H bond by $\text{CpCo}(\text{CO})_2$, $\text{CpRh}(\text{CO})_2$, and $\text{Fe}(\text{CO})_5$ in triethylsilane has been studied. The results are summarized in Scheme 3 and are discussed individually below.

The ultrafast spectra from the 295-nm photolysis of $\text{Fe}(\text{CO})_5$ in triethylsilane solution are presented in Figure 2. After excitation, a single new photoproduct absorbing at 1967 cm^{-1} and what appear to be two highly overlapped bands centered around 1990 cm^{-1} is formed. The kinetic trace of this species exhibits a rise time of 8 ± 1 ps and then decays on a 1200 ± 200 ps time scale as shown in Figure 3.⁵⁵ The cooling of the initially hot photoproduct is responsible for the rise, while the decay of this species and the formation of a small peak at 2016 cm^{-1} is most likely due the formation of the Si–H bond-activated product.⁵⁶ The spectra of the bond-activated product $\text{Fe}(\text{CO})_4(\text{H})(\text{SiEt}_3)$ is shown in the last (long-time) spectrum in Figure 2.

Shown in Figure 4 are the fs-IR spectra of $\text{CpCo}(\text{CO})_2$ in neat Et_3SiH following excitation at 325 nm. At early times the

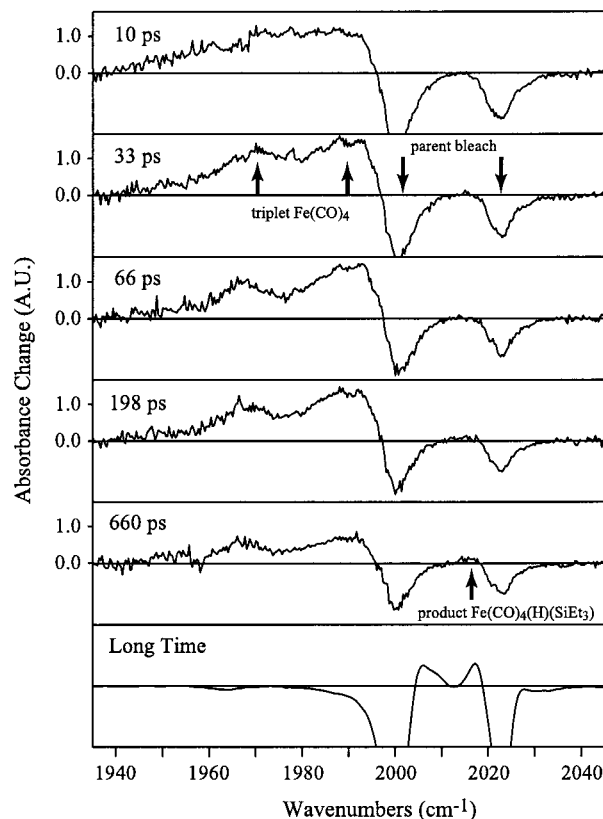


Figure 2. Transient difference spectra in the CO-stretching region for $\text{Fe}(\text{CO})_5$ in neat triethylsilane at 10, 33, 66, 198, and 660 ps and long-time spectra following 295-nm UV photolysis. Under the experimental conditions, the large cross section of the solvent Si–H band ($\sim 2100 \text{ cm}^{-1}$) and the parent CO bands ($2000, 2023 \text{ cm}^{-1}$) make it difficult to access some regions of the spectrum. The long-time spectrum was taken in heptane solution to suppress the formation of di-substituted products due to secondary photolysis.

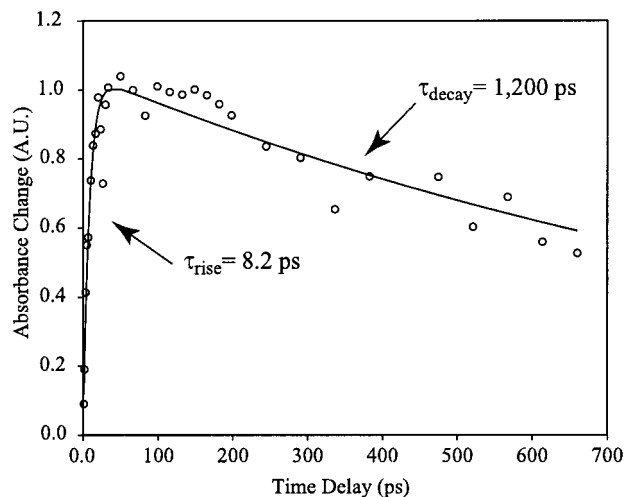


Figure 3. Ultrafast kinetics of $\text{Fe}(\text{CO})_5$ in neat triethylsilane after 295 nm UV photolysis at 1965 cm^{-1} , the CO stretch of the triplet species $\text{Fe}(\text{CO})_4$. The time constants for the exponential fits (solid line) are shown in the graph. The final product is obscured by the parent absorptions and by the Si–H stretch region.

photoproduct peak at 1990 cm^{-1} appears 5 cm^{-1} red-shifted with respect to that of the Si–H bond-activated product at 1995 cm^{-1} . The 1990-cm^{-1} peak appears to completely decay, while the Si–H bond-activated product peak at 1995 cm^{-1} exhibits a rise time of 22 ± 5 ps, as shown in Figure 5. It is difficult to determine whether these dynamics are due to cooling of the

(51) The kinetics of this species are monitored at 1965 cm^{-1} .

(52) Dougherty, T. P.; Heilweil, E. J. *J. Chem. Phys. Lett.* **1994**, *227*, 19.

(53) Dougherty, T. P.; Grubbs, W. T.; Heilweil, E. J. *J. Phys. Chem.* **1994**, *98*, 9396.

(54) Dougherty, T. P.; Heilweil, E. J. *J. Phys. Chem.* **1996**, *100*, 201.

(55) The kinetics of this species are monitored at 1967 cm^{-1} .

(56) Unfortunately, it is difficult to quantify the formation of the product since the product's spectrum is overlapped with the parent as well as the silane Si–H stretch absorption.

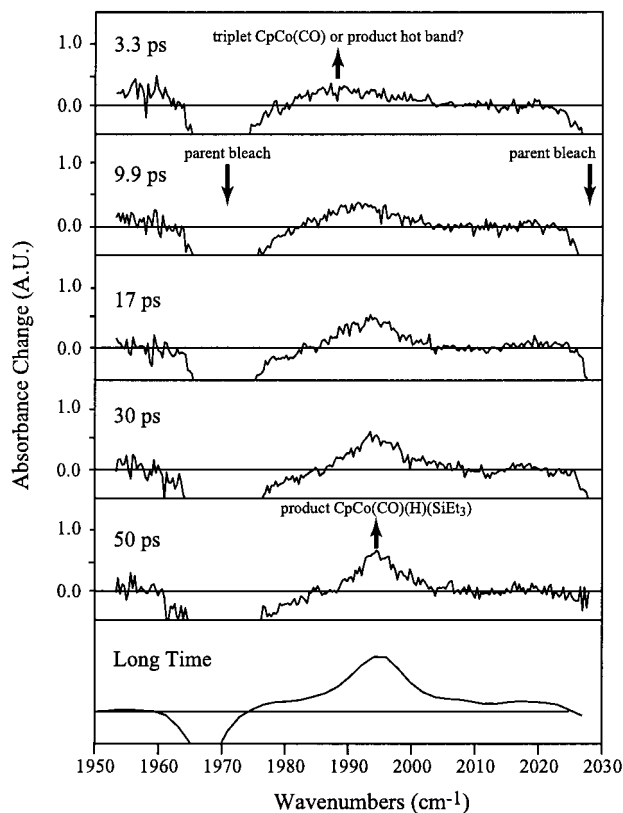


Figure 4. Transient difference spectra in the CO-stretching region for $\text{CpCo}(\text{CO})_2$ in neat silane at 3.3, 9.9, 17, 30, and 50 ps and long-time spectra following 325 nm UV photolysis. The arrows point to the initial species seen at 1990 cm^{-1} and the Si-H activated product at 1995 cm^{-1} .

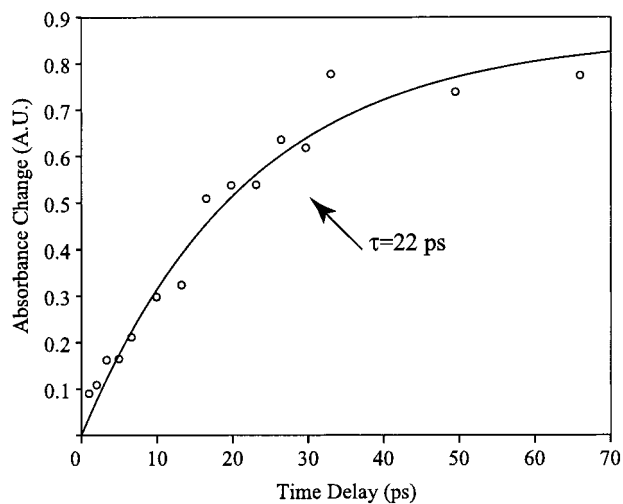


Figure 5. Ultrafast kinetics of $\text{CpCo}(\text{CO})_2$ in neat triethylsilane after 325 nm UV photolysis at 1995 cm^{-1} . The time constant for the exponential fit (solid line) is shown in the graph.

Si-H bond-activated product or the reaction of the nascent photoproduct with the solvent (vide infra). The long-time spectrum of the bond-activated product $\text{CpCo}(\text{CO})(\text{H})(\text{SiEt}_3)$ is shown in the last panel in Figure 4, which clearly indicates that the formation of this product occurs on the ultrafast time scale.

To develop a greater understanding of the reactivity of these photogenerated species, the $\text{CpCo}(\text{CO})_2$ results are compared to studies of isoelectronic $\text{CpRh}(\text{CO})_2$ in triethylsilane. In Figure 6 are the fs-IR spectra of $\text{CpRh}(\text{CO})_2$ in triethylsilane following excitation at 295 nm. At 10 ps a photoproduct peak at 1960 cm^{-1}

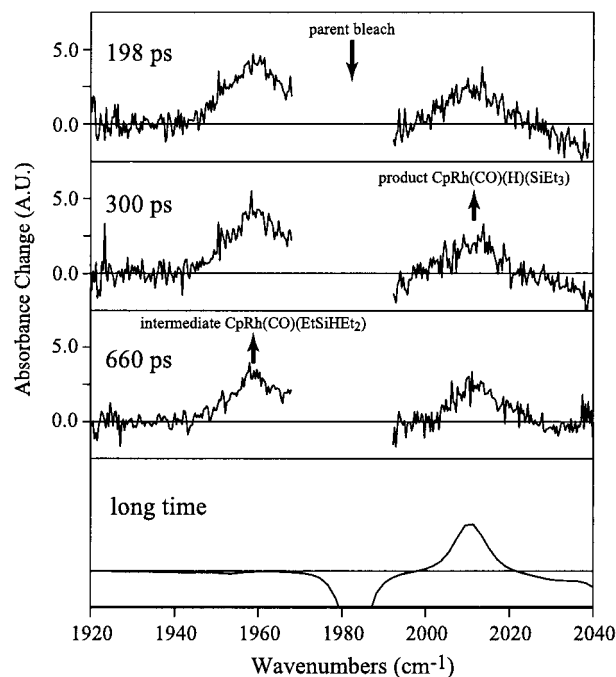


Figure 6. Transient difference spectra in the CO-stretching region for $\text{CpRh}(\text{CO})_2$ in neat triethylsilane, at 198, 300, and 660 ps and long-time spectra after 295 nm UV photolysis.

cm^{-1} and a Si-H bond-activated product band at 2011 cm^{-1} are overlapped with hot bands from the parent; however, the dynamics of this system appear relatively static from 200 to 660 ps. The long-time spectrum of the bond-activated product $\text{CpRh}(\text{CO})(\text{H})(\text{SiEt}_3)$ is shown in the last panel in Figure 6; note the absence of the ethyl-solvated intermediate species peak at 1960 cm^{-1} .

C. DFT and ab Initio Calculation Results. Theoretical calculations have been used to characterize the nature of the transient intermediates under study. The purpose of these calculations is to establish the ground spin state of the intermediates under study and to understand the trends seen in the reactivity of these species.

Geometry Optimizations. The geometries of the parent molecules $\text{CpCo}(\text{CO})_2$ and $\text{Fe}(\text{CO})_5$, the intermediate triplet species, and the final model Si-H bond-activated products are shown in Figures 7 and 8.⁵⁷ The relevant geometric parameters are summarized in Table 1.⁵⁸ The M-CO distances are longer and the CO bond lengths are shorter in the triplet species compared to those in the singlet, which is a general trend seen in several previous calculations.^{2,3,9,10} Triplet $\text{Fe}(\text{CO})_4$ has C_{2v} symmetry, as confirmed in matrix isolation experiments.^{21,59} The theoretical results predict CO-M-CO bond angles of 146° and 99° , while the previous experimental results predict CO-M-CO bond angles of 147° and 120° for triplet $\text{Fe}(\text{CO})_4$ in Ar matrix. The $\text{Fe}(\text{CO})_4$ results are also in good agreement with previous gas-phase theoretical calculations.^{5,60} The calculated singlet and triplet $\text{CpCo}(\text{CO})$ geometries are also very similar to those of Siegbahn.¹⁰ The large increase of the Si-H distances ($\sim 0.76\text{ \AA}$ for $\text{CpCo}(\text{CO})(\text{H})(\text{SiH}_2\text{CH}_3)$ and $\sim 1.28\text{ \AA}$ for Fe -

(57) The MacMolPlt package used for this graphical illustration was obtained from <http://www.msg.ameslab.gov/GAMESS/Graphics/MacMolPlt.shtml>.

(58) The geometry calculation results are provided in full in the supporting Information.

(59) Poliakoff, M. *Chem. Phys. Lett.* **1981**, *78*, 1.

(60) Lyne, P. D.; Mingos, D. M. P.; Ziegler, T.; Downs, A. J. *Inorg. Chem.* **1993**, *32*, 4785.

Table 1. Optimized Geometric Parameters for the Iron and Cobalt Organometallic Systems

compound	Cp-M	M-CO	C-O	M-H	M-Si(C)	Si-H	α^c
Fe(CO) ₅		1.81, 1.82	1.15, 1.15 [1.15, 1.15] ^d				120°, 90°
¹ Fe(CO) ₄		[1.81, 1.83] ^a	1.15				157°, 131°
³ Fe(CO) ₄		1.78, 1.81	1.15				146°, 99°
Fe(CO) ₄ (H)(SiH ₂ CH ₃)		1.79, 1.80	1.15	1.52	2.43	2.77	[147°, 120°] ^d
CpCo(CO) ₂	1.77	1.75 [1.68] ^b	1.15 [1.19] ^b				98°, 99°
¹ CpCo(CO)	1.75	1.75	1.16				95°
³ CpCo(CO)	1.90	1.81	1.15				[98°] ^b
CpCo(CO)(H)(SiH ₂ CH ₃)	1.76	1.74	1.15	1.46	2.27	2.25	138°
							141°
							136°

^a Numbers in brackets are experimental values from ref 72. Parameters for the equatorial CO are given first. ^b Numbers in brackets are experimental values from ref 73. ^c The (CO)-M-(CO) angle. For CpCo(CO)X species, the (CO)-Co-(Cp center) bond angle. ^d From ref 21, Ar matrix results.

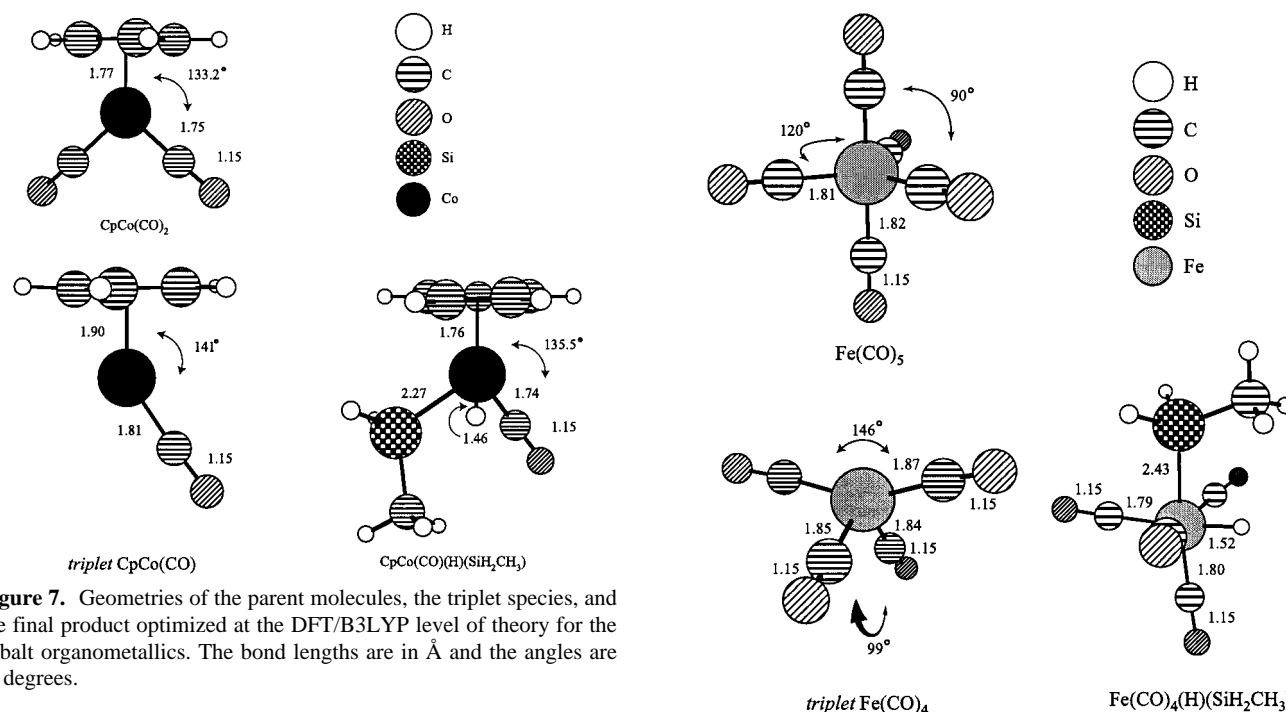


Figure 7. Geometries of the parent molecules, the triplet species, and the final product optimized at the DFT/B3LYP level of theory for the cobalt organometallics. The bond lengths are in Å and the angles are in degrees.

(CO)₄(H)(SiH₂CH₃) in the bond-activated products' geometry optimizations indicate that the Si-H bond is almost totally broken in these species.

Energy Calculations. While the absolute thermochemical errors of this theoretical model are on the order of ~5 kcal/mol,³⁷ all of the computational results are presented as relative energies, which represent a more meaningful quantity in comparative situations. The calculated singlet metal-ligand interaction energies are listed in Table 2. All binding energies have been calculated at the MP2 level of theory using the DFT geometries.⁶¹ The calculated binding energies of ethane qualitatively demonstrate the stability of the singlet metal-alkane interaction and allow for a comparison between the different organometallics. The calculated binding strengths for various other ligands are also presented.

The results of the DFT and pt2-mcscf calculations for the singlet and the triplet species are shown in Table 3. The DFT and pt2-mcscf results predict a lower energy for the triplet state relative to that of the singlet for CpV(CO)₃, CpMn(CO)₂, Fe(CO)₄, and CpCo(CO). While the pt2-mcscf calculation

(61) The calculations of the singlet/alkyl complexes are likely to be underestimated due to the fact that the interaction energy between a transition metal and a series of chain alkanes may increase with chain length. See Ishikawa, Y.; Brown, C. E.; Hackett, P. A.; Rayner, D. M. *Chem. Phys. Lett.* **1988**, *150*, 506.

Figure 8. Geometries of the parent molecules, the triplet species, and the final product optimized at the DFT/B3LYP level of theory for the iron organometallics. The bond lengths are in Å and the angles are in degrees.

predicts a slightly more stable triplet CpRh(CO), DFT calculation shows that singlet CpRh(CO) is energetically more favorable. Experimental evidence, such as the C-H bond-activation ability of CpRh(CO), also suggests that this species has a singlet ground state.

To understand the reactivity of these triplet species, the metal-Si coordinate potential energy curves were calculated at the DFT level of theory.⁶² The results are shown in Figure 9 and are summarized in Tables 4 and 5. The triplet/singlet Fe(CO)₄ and CpV(CO)₃ crossover points occur at metal-Si distances of 3.85 and 4.34 Å, respectively. The iron complex crossover is 1.73 kcal/mol above the (unsolvated) triplet ground state, while the vanadium barrier is 1.56 kcal/mol. The CpCo(CO)/model silane calculation results show that this triplet species has a slight attractive interaction with the model silane solvent. The -0.71 kcal/mol well of this interaction occurs at a metal-Si distance of 3.2 Å. The singlet/triplet crossover occurs

(62) These species were studied because they form stable triplet species in alkane, while the lifetimes are much shorter in triethylsilane solution (the same is not true for the manganese complex).

Table 2. Binding Strengths of Various Organometallic Fragment Species with Co, C₂H₃, and SiH₃CH₃ Model Ligands^a

fragment	ligand	ΔE (kcal/mol)
CpV(CO) ₃	CO	42.1 ^b
CpMn(CO) ₂		64.6
Fe(CO) ₄		67.3 (ax), 52.2 (eq)
CpCo(CO)		60.8
CpRh(CO)		51.0
CpV(CO) ₃	C ₂ H ₆	3.55 ^b
CpMn(CO) ₂		7.71
Fe(CO) ₄		6.93
CpCo(CO)		12.3
CpRh(CO)		9.18 ^c
CpV(CO) ₃	SiH ₂ CH ₃	16.0
CpMn(CO) ₂		54.2
Fe(CO) ₄		90.9
CpCo(CO)		115
CpRh(CO)		162

^a All energies are in kcal/mol. ^b From ref 2. ^c The nonactivated complex.

Table 3. Energetic Splitting between Singlet and Triplet States at Various Levels of Theory

(ground state)- organometallic	ΔE^a — (DFT) kcal/mol	ΔE^a (pt2-mcscf) kcal/mol	vert.- ΔE^b (pt2-mcscf) kcal/mol
(triplet)-CpV(CO) ₃	3.10 ^c	22.3	28.4
(triplet)-CpMn(CO) ₂	4.69	10.4	27.5
(triplet)-Fe(CO) ₄	5.43	6.29	19.5
(triplet)-CpCo(CO)	25.9	20.5	23.3
(singlet)-CpRh(CO)	-0.38	3.11	4.49

^a Calculated as $E(\text{ground spin state}) - E(\text{excited spin state})$. ^b The ΔE between the ground and excited spin state at the ground-state geometry. ^c From ref 2.

at a metal–Si distance of 2.5 Å which is 0.73 kcal/mol above the (unsolvated) triplet ground state. Spin–orbit coupling (SOC) calculations at the ground-state triplet geometry were also performed using the optimized multiconfigurational wave function and are summarized in Table 4. Overall, the coupling constant is much greater for the vanadium, manganese, and cobalt complexes than that of the iron system.

IV. Discussion

The experimental and theoretical results of the present and past investigations establish that the solution-phase dynamics upon photolysis of CpCo(CO)₂ and Fe(CO)₅ are due to the exclusive formation of triplet intermediates. In triethylsilane, these triplet intermediates form the Si–H bond-activated product on the ultrafast time scale, while the photogenerated singlet CpRh(CO) species' reactivity is overall much slower. A change in the Si–H bond-activation mechanism between the triplet and singlet is responsible for these observations.

A. Liquid-Phase Photolysis of CpCo(CO)₂, Fe(CO)₅, CpMn(CO)₃. The Dynamics of Triplet Intermediates. The ultrafast photochemistry of CpCo(CO) in alkane solution was studied by Dougherty et al.⁶³ Our results are consistent with their report; an intermediate peak appears at 1990 cm⁻¹ and does not decay within 660 ps, the maximum pump–probe time delay of our experimental apparatus. This intermediate is most likely triplet CpCo(CO), as the DFT frequency analyses support the spectral assignment,⁶⁴ and the DFT and pt2-mcscf predict large triplet–singlet energy splittings favoring the triplet ground state. As Bengali et al. showed, this species does not interact

(63) Dougherty, T. P.; Heilweil, E. J. *J. Chem. Phys.* **1994**, *100*, 4006.

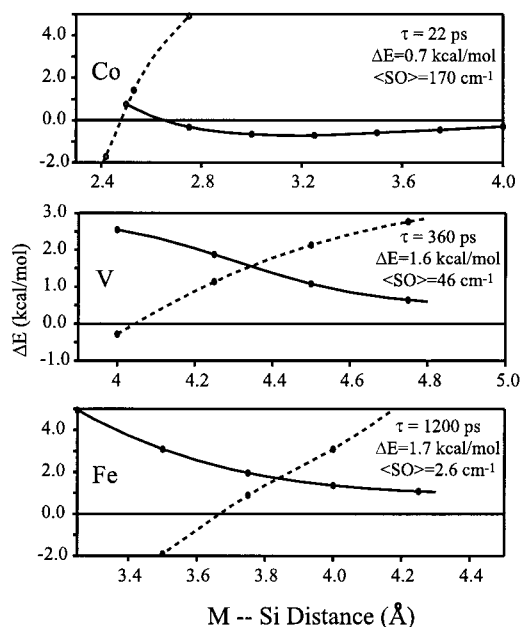


Figure 9. Results of the DFT singlet and triplet organometallic/SiH₃CH₃ energy calculations. The curves are generated by performing a geometry optimization at a fixed metal–Si bond length for each organometallic system. The singlet potential curves are represented by dashed lines, and the triplet curves have solid lines. The lines are spline fits to the data (circles) and are presented for visualization purposes only.

with alkanes, which is also consistent with the formation of a triplet intermediate.¹⁷

While this species is stable in heptane, triplet CpCo(CO) is overall the most reactive of all (triplet or singlet) species under study in triethylsilane. In triethylsilane, a peak at 1990 cm⁻¹ appears at early times and decays with the concomitant formation of a new product peak at 1995 cm⁻¹ in 22 ps. Compared to the long-time spectrum in Figure 4, the 1995 cm⁻¹ peak is due to the bond-activated product CpCo(CO)(H)(SiEt₃). It is unclear whether the decay of peak at 1990 cm⁻¹ is due to cooling of a bond-activated product hot band or the reaction of the triplet species with the triethylsilane solvent; however, the 1990 cm⁻¹ peak is most likely the nascent triplet species as this peak position coincides with the triplet photoproduct in heptane. Regardless, the reactivity of triplet CpCo(CO) in triethylsilane is very fast with the Si–H bond-activated product appearing at a rate of $k \geq 4.5 \times 10^{10} \text{ s}^{-1}$. A similar fast reactivity was also observed by Dougherty et al. for CpCo(CO) in 1-hexene.⁶³ These results are summarized in Schemes 2 and 3.

In dry heptane, the photochemistry of Fe(CO)₅ appears very similar to that of CpCo(CO)₂. Instantaneous parent bleaches are accompanied by the formation of a single new photoproduct absorbing at 1965 cm⁻¹ and overlapping bands centered at 1987 cm⁻¹, which does not decay within the maximum pump–probe time delay of 660 ps. This photoproduct is most likely triplet Fe(CO)₄ as the DFT and ab initio calculations predict a triplet ground state, and the experimental photoproduct frequencies are similar to those of the triplet species seen in matrix experiments.^{59,65} The Fe(CO)₄ intermediate has been shown to have

(64) The DFT frequency calculations for the triplet species (2121 cm⁻¹) and the parent CpCo(CO)₂ (2085 and 2124 cm⁻¹) mirror the trends seen in the data, while the theoretical calculations predict that the alkyl-solvated singlet carbonyl stretch frequency (2067 cm⁻¹) would appear to the red of the parent absorptions.

(65) Zhou, M. F.; Chertihin, G. V.; Andrews, L. *J. Chem. Phys.* **1998**, *109*, 10893.

Table 4. Results of the DFT Potential Energy Curve Calculations^a

complex/ SiH ₃ CH ₃	minimum (Å)	interaction <i>E</i> (kcal/mol)	singlet/triplet crossover (Å)	barrier (kcal/mol)	SOC (cm ⁻¹)	τ (silane) (ps)
CpCo(CO)	3.2	-0.71	2.5	0.73	170	22
CpV(CO) ₃	—	—	4.3	1.56	46.2	340
Fe(CO) ₄	—	—	3.9	1.73	2.55	1200
CpMn(CO) ₂ ^b	—	—	—	—	232	105 ^c

^a The potential minimum data are reported for triplet CpCo(CO)/SiH₃CH₃. The singlet/triplet spin-orbit constants and the triplet species lifetimes in triethylsilane solution are also summarized. ^b The potential curves for singlet and triplet CpMn(CO)₂/SiH₃CH₃ were not calculated, as this species is unstable in alkane as well as in triethylsilane solution. ^c From ref 3.

Table 5. Summary of the Observed Vibrational Frequencies, DFT Results, and Literature References (in parentheses)

complex	observed frequency (cm ⁻¹)	DFT frequency ^a (cm ⁻¹)	reference
Fe(CO) ₅	2023, 2000 heptane	2124, 2100	2024, 2004 C ₆ D ₆ (74)
³ Fe(CO) ₄	1987, 1965 heptane	2102, 2093	1993/2, 1985, 1967 CH ₄ matrix (21)
Fe(CO) ₄ (H)(SiEt ₃)	2091, 2017, 2006 heptane ^b	2171, 2131, 2126, 2112	2093, 2028, 2018, 2007 hexane ^c (75)
CpCo(CO) ₂	2031, 1971 heptane	2124, 2085	2031, 1971 <i>n</i> -hexane (63)
³ CpCo(CO)	1990 heptane	2121	1993 <i>n</i> -hexane (63)
CpCo(CO)(H)(SiEt ₃)	1995 triethylsilane	2105	this work
CpRh(CO) ₂	2047, 1984 triethylsilane	2129, 2077	2048, 1985 cyclohexane (76)
¹ CpRh(CO)(EtSiHEt ₂)	1960 triethylsilane	2059	1963 ^d cyclohexane (76)
CpRh(CO)(H)(SiEt ₃)	2011 triethylsilane	2101	2010 <i>n</i> -pentane (77)

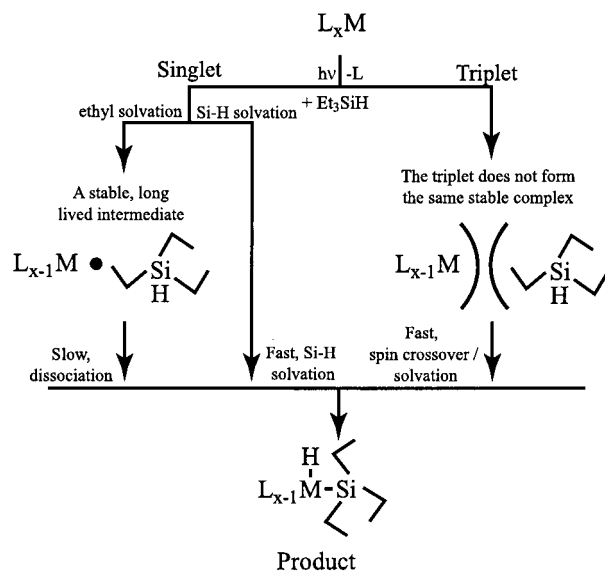
^a Data are for the model compounds and are necessarily gas-phase data. The DFT calculated frequencies are generally known to be blue-shifted from the experimental values, see ref 79. ^b A fourth peak is likely overlapped with the 2023 cm⁻¹ Fe(CO)₅ parent bleach. ^c The spectral data are for Fe(CO)₄(H)(SiMe₃). ^d The spectral data are for CpRh(CO)(cyclohexane).

weak interactions with alkanes,⁶⁶ which is also consistent with the formation of a triplet species. Consequently, triplet Fe(CO)₄ is the only intermediate formed under the experimental conditions. In triethylsilane, the same triplet photoproduct appears at 1967 and 1990 cm⁻¹. The reaction time scale in neat triethylsilane is approximately 1200 ± 200 ps, based upon the decay kinetics of the initially formed triplet species and the coincident formation of the Si-H activated product. The Fe(CO)₄ reaction rate of $k = 8.3 \times 10^8$ s⁻¹ is the slowest of the triplet species under investigation in triethylsilane. These results are also summarized in Schemes 2 and 3.

The formation and the decay of the photoproducts of CpMn(CO)₃ in alkane solution were studied to compare the results to the triethylsilane studies. In contrast to the long-time stability of the triplet intermediates of CpV(CO)₃, Fe(CO)₄, and CpCo(CO) in alkane solution, the triplet kinetics of CpMn(CO)₂ show a 119 ps decay with a corresponding increase in the singlet alkyl solvate, as summarized in Scheme 2. The difference is likely due to the large spin-orbit coupling of CpMn(CO)₃, the relatively low triplet/singlet energy gap, as well as the calculated stabilizing interaction enthalpy of the singlet manganese alkyl solvate compared to those of the other species.

The results for these triplet species may be summarized as follows. Upon photolysis of CpCo(CO)₂ and Fe(CO)₅ in solution, a single carbonyl is lost, and the photoproducts are in

(66) Nayak, S. K.; Burkey, T. J. *J. Am. Chem. Soc.* **1993**, *115*, 6391.

Scheme 4. Overall Si-H Bond-Activation Mechanism by Singlet and Triplet Coordinatively Unsaturated Organometallic Species

the unsolvated ground triplet state. These species are stable in alkane solution yet react in triethylsilane solution on the ultrafast time scale. These results are similar to the previous results for triplet CpV(CO)₃ and CpMn(CO)₂, although triplet CpMn(CO)₂ is unstable in alkane as well as in triethylsilane solution.

B. Liquid-Phase Photolysis CpRh(CO)₂. The Dynamics of a Singlet Intermediate. The situation is very different for the photochemistry of CpRh(CO)₂. It has been established that CpRh(CO) has a singlet ground state^{9,10} and that singlet organometallic species have greater interactions with alkanes than triplet species.^{10,17-20} In triethylsilane solution, previous results have shown that singlet intermediates may coordinate to the ethyl moiety of triethylsilane, which form long-lived intermediates.^{2,4,67} This ethyl solvate does not form the final Si-H bond-activated product until this complex has dissociated as shown in Scheme 4.⁶⁷

As seen in Figure 6, the dynamics of the photoproduct CpRh(CO) absorbing at 1960 and 2011 cm⁻¹ appear to remain relatively constant from 200 to 660 ps. The species at 1960 cm⁻¹ can be assigned to the triethylsilane ethyl-moiety solvate of singlet CpRh(CO),⁶⁸ and the 2011 cm⁻¹ peak corresponds to the Si-H bond-activated product as seen in the long-time spectrum of Figure 6. The lifetime of the CpRh(CO) ethyl

(67) Kotz, K. T.; Yang, H.; Snee, P. T.; Payne, C. K.; Harris, C. B. *J. Organomet. Chem.* **2000**, *596*, 183.

(68) This assignment is in agreement with theory as the DFT frequency results for the singlet (unactivated) alkyl solvate (2059 cm⁻¹) and the parent CpRh(CO)₂ (2077 and 2129 cm⁻¹) agree with the trends seen in the data, while the calculated unsolvated triplet species absorption (2089 cm⁻¹) is not consistent with the experimental results. The DFT as well as previous calculations have shown that the singlet is the ground state. See ref 76 for the frequency assignment.

moiety must be rather long-lived as the overall first-order bond-activation rate was extrapolated to be $k = 2.7 \times 10^3 \text{ s}^{-1}$ in the concentration-dependent study of Belt et al.,⁶⁹ however, the final formation of the product may be further slowed due to activation of the C–H bond of the alkyl moiety.⁷⁰ Unfortunately, the low signal due to the 25% quantum yield of CpRh(CO)₂ makes a detailed kinetic analysis of the initial formation of the Si–H bond-activated product impractical with the present femtosecond apparatus.

These experimental results can be summarized as follows. The monocarbonyl photoproduct of CpRh(CO)₂ in triethylsilane is a singlet, forming a long-lived ethyl moiety solvated species and the Si–H bond-activated product within 10 ps. The ethyl-solvated singlet forms the final bond-activated product on a time scale several orders of magnitude longer than the Fe(CO)₄ and CpCo(CO) triplet species. These results are similar to our previous studies of triplet/singlet CpV(CO)₃ and CpMn(CO)₂ in triethylsilane, in which it was shown that the triplet species decays faster than the ethyl-solvated singlet to form the final bond-activated product.

C. The Reaction Mechanisms. In triethylsilane solution, coordinatively unsaturated singlet intermediates may form the Si–H bond-activated product via Si–H solvation on the ultrafast time scale; however, the singlet species also becomes trapped in an ethyl moiety solvated state. The singlet ethyl solvate does not form the final bond-activated product until the ethyl-solvated organometallic has dissociated.⁶⁷ As the experimental and theoretical results have established that triplet coordinatively unsaturated intermediates do not interact with alkanes, they do not coordinate with the ethyl moiety of triethylsilane and are thus free to form the final Si–H bond-activated product along a much faster time scale. It is interesting to note that in 1974 Poliakov and Turner put forth the same argument in comparing the reactivity of ³Fe(CO)₄ versus ¹Cr(CO)₅ toward various ligands²¹ and concluded that Cr(CO)₅ is the more reactive of the two toward alkanes. Likewise, Siegbahn used a similar mechanism to explain the differences observed in the reactivity of CpRh(CO) and CpCo(CO) with CO in alkane solution.¹⁰ As previously proposed, the triplet reactivity can be attributed to a solvation/spin crossover by the strong coupling site of the reactant.^{2,3} The conclusions are summarized in Scheme 4, the proposed mechanism for Si–H bond-activation of triethylsilane with singlet and triplet coordinatively unsaturated organometallic complexes.

D. Understanding the Trends of Triplet Reactivity. It has been shown that the iron, cobalt, and vanadium organometallic complexes form stable triplet intermediates in alkane yet decay on the ultrafast time scale in triethylsilane. The trend of the reactivity in triethylsilane from Table 4 is CpCo(CO) > CpV(CO)₃ > Fe(CO)₄. These experimental results may be interpreted in terms of two factors: the barrier at the singlet/triplet curve crossover and the calculated coupling of the singlet and triplet surfaces.

The trends in the reactivity of these species may be understood in terms of the approximate nonadiabatic potential energy surfaces generated by the DFT singlet and triplet organometallic/model silane calculations in Figure 9. The singlet state (dashed) curves for all of the species slope downhill with decreasing M–Si distance, which shows that the singlet Si–H

bond-activated product is overall the most favorable species energetically. The triplet (solid) curves, however, show that the triplet species' interaction with SiH₃CH₃ is generally unfavorable. These theoretical calculations elucidate the fast reactivity of triplet CpCo(CO) in triethylsilane. In this system, there exists a small classical barrier at the singlet/triplet crossover due to what appears to be a small attractive interaction between the triplet cobalt species and the model silane solvent. The triplet species metal–Si minimum is less than 1 Å from the singlet activated product bond length, which indicates that only a slight rearrangement is necessary to form the product. At the triplet minimum, the spin–orbit calculation shows a strong coupling between the triplet and singlet surfaces. This result is important as the spin–orbit coupling is responsible for intersystem crossing.⁷¹ Consequently, the low classical barrier as well as the large coupling between states explains why such a fast ($k \geq 4.5 \times 10^{10} \text{ s}^{-1}$) reaction occurs between triplet CpCo(CO) and the Si–H bond.

There does not appear to be an attractive interaction of triplet Fe(CO)₄ and triplet CpV(CO)₃ with SiH₃CH₃, which results in a larger classical barrier at greater crossing-point distances than seen in triplet CpCo(CO). The reactivity of these species may be understood in two limiting regimes. The vanadium triplet species has a significant singlet/triplet coupling; however, this species also has a larger classical barrier to activation than the cobalt complex. The Fe(CO)₄ intermediate, which reacts with triethylsilane at the slowest rate of all the triplets species, has an activation barrier similar to that of CpV(CO)₃ yet has a very small coupling between the spin states. We can conclude that knowledge of the spin–orbit strengths as well as the potential energy surfaces are necessary in understanding the reactivity of these species.

V. Conclusions

We have shown in this paper that the photochemical reaction dynamics of Fe(CO)₅ and CpCo(CO)₂ are due to the formation of triplet-state intermediates. The results are in contrast to the singlet intermediate dynamics seen with CpRh(CO)₂. Due to a change in the reaction mechanism, the overall reactivity of the triplet species is much greater than that of similar singlet species.

A general mechanism explaining the reactivity of triplet organometallics may now be proposed. Coordinatively unsaturated singlet organometallics will tend to associate to most solvents, even alkanes. These interactions will likely hinder further reactivity with a stronger coupling site as these alkyl-solvated species may exist for milliseconds in solution. The triplet species are free to react at a faster rate as they do not coordinate to the same degree with a weak coupling alkyl site. The time scale of the triplet metal complex reactivity can be understood in terms of spin–orbit coupling between the singlet and triplet surfaces as well as the classical barrier to bond-activation. This mechanistic change explains the differing

(71) Poli, R. *Chem. Rev.* **1996**, *96*, 2135.

(72) Beagley, B.; Schmidling, D. G. *J. Mol. Struct.* **1974**, *22*, 466.

(73) Beagley, B.; Parrott, C. T.; Ulbrecht, G. G.; Young, J. J. *J. Mol. Struct.* **1979**, *52*, 47.

(74) Church, S. P.; Grevels, F.-W.; Hermann, H.; Kelly, J. M.; Klotzbucher, W. E.; Schaffner, K. J. *J. Chem. Soc., Chem. Commun.* **1985**, 594.

(75) Krentz, R.; Pomeroy, R. K. *Inorg. Chem.* **1985**, *24*, 2976.

(76) Asbury, J. B.; Ghosh, H. N.; Yeston, J. S.; Bergman, R. G.; Lian, T. *Organometallics* **1998**, *17*, 3417.

(77) Drolet, D. P.; Lees, A. J. *J. Am. Chem. Soc.* **1992**, *114*, 4186.

(78) Asplund, M. C. *Time-Resolved Infrared Studies of C–H Bond Activation by Organometallics*; University of California at Berkeley, 1998; p 67.

(79) Scott, A. P.; Radom, L. *J. Phys. Chem.*, **1996**, *100*, 16502.

(69) Belt, S. T.; Grevels, F.-W.; Klotzbucher, W. E.; McCamley, A.; Perutz, R. N. *J. Am. Chem. Soc.* **1989**, *111*, 8373.

(70) This is reasonable in light of the fact that CpRh(CO) has been found to activate the C–H bond in less than 30 ns in cyclohexane,⁷⁸ and is stable in solution for 100 ms.⁶⁹ In fact, the small decay in the 1960 cm⁻¹ peak may be due to C–H activation of the ethyl moiety.

reactivity of triplet and singlet coordinatively unsaturated organometallic complexes in triethylsilane and can likely be extended to other chemical systems.

Acknowledgment. This work was supported by a grant from the National Science Foundation. We also acknowledge equipment used under the Office of Basic Energy Science, Chemical Science Division, U.S. Department of Energy Contract DE-AC03-76SF00098. We thank Professor C. B. Moore for the use of the static FTIR spectrometer; Professor A. P. Alivisatos for the use of a UV-vis spectrometer; Mr. J. Yeston and Ms. S.

Mebane for assistance with handling of the samples and Mr. T. Van Voorhis for helpful discussions. We also thank Professor T. Don Tilley for the gift of an inert-atmosphere glovebox.

Supporting Information Available: The DFT/B3LYP optimized geometries for all the species under investigation are provided (PDF). This material is free of charge via the Internet at <http://pubs.acs.org>.

JA002350R